Front. Optoelectron. 2015, 8(3): 282–288
DOI 10.1007/s12200-015-0529-4

RESEARCH ARTICLE

Building one-dimensional Bi_2S_3 nanorods as enhanced photoresponding materials for photodetectors

Taotao DING[1], Yu TIAN[2], Jiangnan DAI[1], Changqing CHEN (✉)[1]

1 Wuhan National Laboratory for Optoelectronics, Huazhong University of Science and Technology, Wuhan 430074, China
2 School of Physics and Information Engineering, Jianghan University, Wuhan 430056, China

Abstract In this paper, Bi_2S_3 nanorods were successfully synthesized via a facile one-pot hydrothermal method and characterized by X-ray diffraction, field emission scanning electron microscopy, transmission electron microscopy and X-ray photoelectron spectroscopy. Then the Bi_2S_3 nanorods were deposited on Au interdigital electrodes by dip-coating to fabricate photodetectors. The photoresponse properties using Bi_2S_3 nanorods as a representative system showed a significantly enhanced conductivity and the current-voltage (*I-V*) characteristic exhibited about ca. 2 orders of magnitude larger than the dark current. The response and decay time was estimated to be ~371.66 and 386 ms, respectively, indicating Bi_2S_3 may be an excellent candidate for high speed and high-sensitivity photoelectrical switches and light sensitive devices.

Keywords Bi_2S_3, nanorods, photoresponse property, photodetector

1 Introduction

In recent years, various morphologies of nanostructures, including one dimensional (1D) nanoribbons/nanowires [1,2] and nanorods [3], two dimensional (2D) nanosheets [4], and three dimensional (3D) hierarchically complex architectures [5–7] have been fabricated. Among them, 1D nanostructured material is believed to play an important role in the next-generation building blocks for electronic devices [8], solar cells [9–11], photocatalysis [12], lithium-ion batteries [13] and piezoelectric nanogenerators [14] for their high surface-to-volume ratio and excellent electron transport property. As an important member of bismuth chalcogenides (Bi_2S_3, Bi_2Se_3, and Bi_2Te_3), bismuth sulfide (Bi_2S_3) has drawn increasing attention in solar cells [15], photo-detectors [16–18], gas sensors [19], Schottky diode [20], lithium-ion battery [21], X-ray computed tomography imaging (CT) [22], and thermoelectric devices [23]. Actually, Bi_2S_3 has also been considered as one of the most promising materials for photoactive materials due to its low band gap, high absorption coefficients and reasonable energy conversion efficiency. In view of the high surface area, high crystal quality for fast electron separation and transport, Bi_2S_3 nanostructure has been used as an efficient photoactive material more frequently [15]. It is well known that photoresponse properties are largely determined by morphology, and many approaches have been proposed to synthesize various Bi_2S_3 nanostructures, such as microwave irradiation [24], chemical vapor deposition (CVD) method [25–27], anodized alumina membrane method [28], sonochemical approach [29], solvothermal process [30], electrochemical deposition [31] and biomolecule-assisted route [32]. Compared with the approaches mentioned above, hydrothermal process [16] is a more facile, low-cost and easy route to obtain Bi_2S_3 nanostructures with high crystallinity.

Herein, in this paper, Bi_2S_3 nanorods were successfully prepared via a one-pot and surfactant-free hydrothermal method. Typically, $Bi(NO_3)_3$, thiourea (TU) and ethylenediaminetetraacetic acid disodium salt (EDTA) were used as starting materials to obtain the Bi_2S_3 nanorods structures. The current-voltage (*I-V*) characteristic of optical switches based on Bi_2S_3 nanorods have been improved significantly, which exhibited ca. 2 orders of magnitude larger than the dark current. This result suggests an enhanced conductivity and high sensitivity of Bi_2S_3 nanorods based photodetectors. Furthermore, the response and decay time of the photodetector was estimated to be ~371.66 and 386 ms, respectively. These results indicate that the Bi_2S_3 nanorod is a promising candidate material for photoelectrical witches and light sensitive devices.

Received May 5, 2015; accepted June 11, 2015

E-mail: cqchen@hust.edu.cn

2 Experiment

2.1 Materials synthesis

$Bi(NO_3)\cdot 5H_2O$, TU, EDTA, ammonium hydroxide ($NH_3\cdot H_2O$) were purchased from Sinopharm Chemical Reagent Co., Ltd. (Shanghai) without further purification.

In a typical procedure, 1.22 g $Bi(NO_3)\cdot 5H_2O$, 0.57 g TU and 0.66 g EDTA were added successively into 60 mL distilled water, followed with ammonium hydroxide to adjust pH to 8. A clear solution was obtained with assistant of sonication, which was then transferred into a 100 mL teflon-lined autoclave and heated at 130°C for 9 h. Finally, the product was collected and washed with distilled water and ethanol for three times, and dried at 60°C for 12h in an vacuum oven.

The morphologies, structures and composition were characterized by field emission scanning electron microscopy (FE-SEM, FEI Nova NanoSEM 450), transmission electron microscopy (TEM, FEI Tecnai G20). X-ray powder diffraction (XRD) characterization were performed on Shimadzu XRD-7000s diffractometer equipped with Cu Kα radiation (λ = 0.15418 nm). X-ray photoelectron spectra (XPS) were characterized with Kratos AXIS Ultra DLD-600W X-ray photoelectron spectroscopy.

2.2 Device fabrication

The photodetectors were fabricated by a simple drop-casting method. Typically, 10 mg Bi_2S_3 nanorodswas first suspended in 2 mL ethanol by sonication. The Au interdigital electrodes on Al_2O_3 substrates were cleaned by distilled water, ethanol and acetone successively for 15 min, respectively. And then 10 μL of suspension was dropped on the Au electrodes. Finally, the devices were put in an oven at 30°C for 12 h. Electrical property measurements and light sensing tests were conducted in ambient condition by a semiconductor characterization system (Keithley 2420) and a solar simulator (Newport 91160-1000) in the dark and under simulated AM 1 and 1.5 illumination.

3 Results and discussion

3.1 Crystal structure

The XRD pattern of the as prepared Bi_2S_3 nanorods can be found in Fig. 1(a). Clearly, all the diffraction peaks can be indexed as the orthorhombic phase of Bi_2S_3 (JCPDS No.

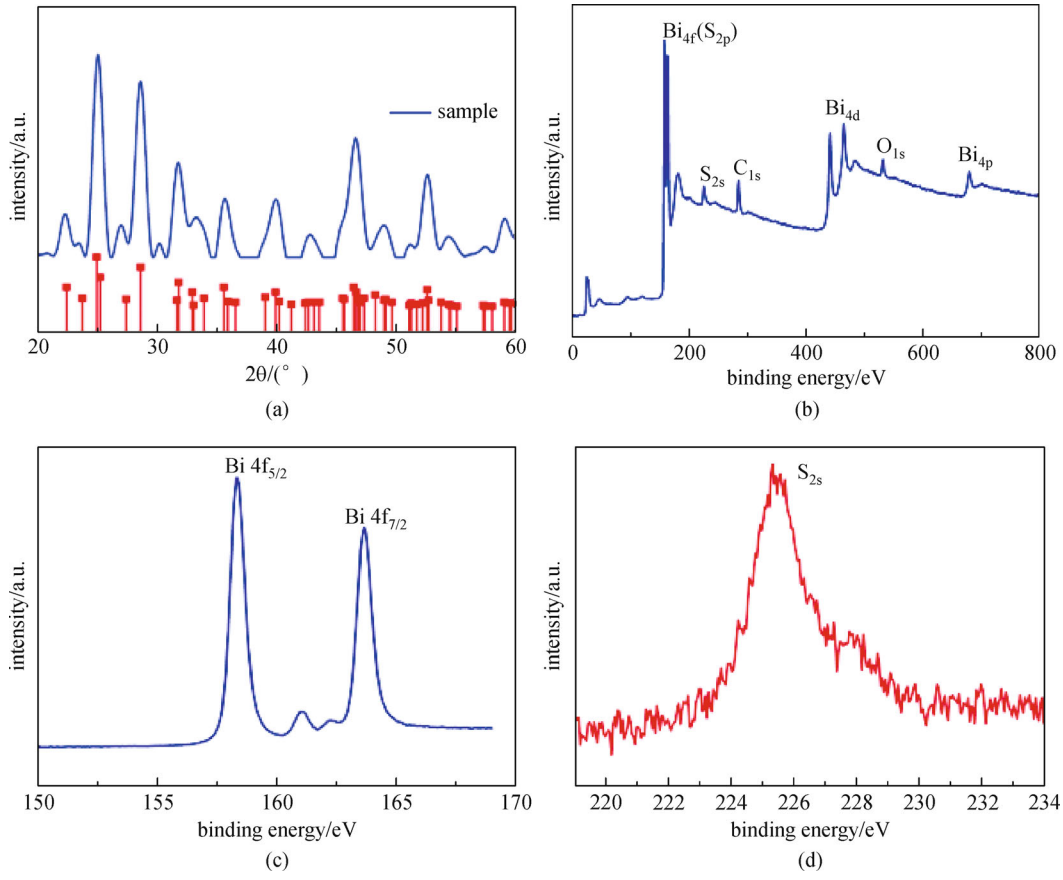

Fig. 1 (a) XRD pattern of the Bi_2S_3 nanorods. The pattern shown at bottom is the standard XRD card of Bi_2S_3 (JPCDS no. 17-0320); (b), (c) and (d) the full spectra, Bi 4f and S 2s region of the XPS spectrum of Bi_2S_3 nanorods, respectively

17-0320) with cell constants $a = 3.981$, $b = 11.147$ and $c = 11.305$. The Bi-EDTA precursors were entirely decomposed after the hydrothermal reaction without any characteristic peaks. In another investigation, the average crystalline size was derived from the Scherrer formula as shown below:

$$D = \frac{k\lambda}{B\cos\theta},$$

where D is the average crystalline size, k is a constant whose value is typically 0.9 for non-spherical crystals, B is the full width at half maximum (FWHM) of the diffraction peak (in radians) that has the maximum intensity in the diffraction pattern, λ is the wavelength of incident X-ray beam (0.154184 nm), and θ is diffraction angle or Bragg angle. From this formula, the average crystalline size of Bi_2S_3 was calculated to be 28.26 nm.

The chemical composition of the Bi_2S_3 was further analyzed by XPS, as shown in Fig. 1(b). The main peaks could be indexed to Bi 4f, S 2s, O 1s and C 1s regions, which implied that no other metallic or inorganic containments were involved in the outcomes. The peaks of O could be attributed to the O_2, CO_2 and H_2O absorbing on the surface of the sample, which is common for powders exposed to the atmosphere and more pronounced for ultrafine powders with high surface areas. Figure 1(c) presents high resolution XPS spectra of Bi 4f in Bi_2S_3 nanorods. The Bi 4f spectrum exhibits spin-orbit splitting into $4f_{5/2}$ (163.65 eV) and $4f_{7/2}$ (158.3 eV) components, and both contained the same chemical information. As illustrated in Fig. 1(d), the peak measured in the S energy region detected at 225.3 eV can be attributed to the S 2s transition.

3.2 Morphology of Bi_2S_3 sample

The SEM morphologies of the obtained Bi_2S_3 nanorods are shown in Figs. 2(a) and 2(b). It can be clearly seen that nanorods are dispersed in the field of version. The length and the diameter of the nanrodsareca. 0.5–1 μm and 70–100 nm, respectively. TEM and HRTEM were employed to get further information about the morphology of the obtained Bi_2S_3 nanorods. Figure 2(c) is a TEM image of a single Bi_2S_3 nanorod radiating from the center; it can be found that the surface of the individual nanorod is smooth. Figure 2(d) shows the HRTEM image of the individual nanorod. The single nanorod exhibits a lattice spacing of 0.79 nm, correspond to the (110) plane of orthorhombic Bi_2S_3. The TEM results are consistent with those reported for the Bi_2S_3 nanostructures previously, which are scribed to the highest surface energy of the (001) plane as well as the strongest bond energy of the c axis [33].

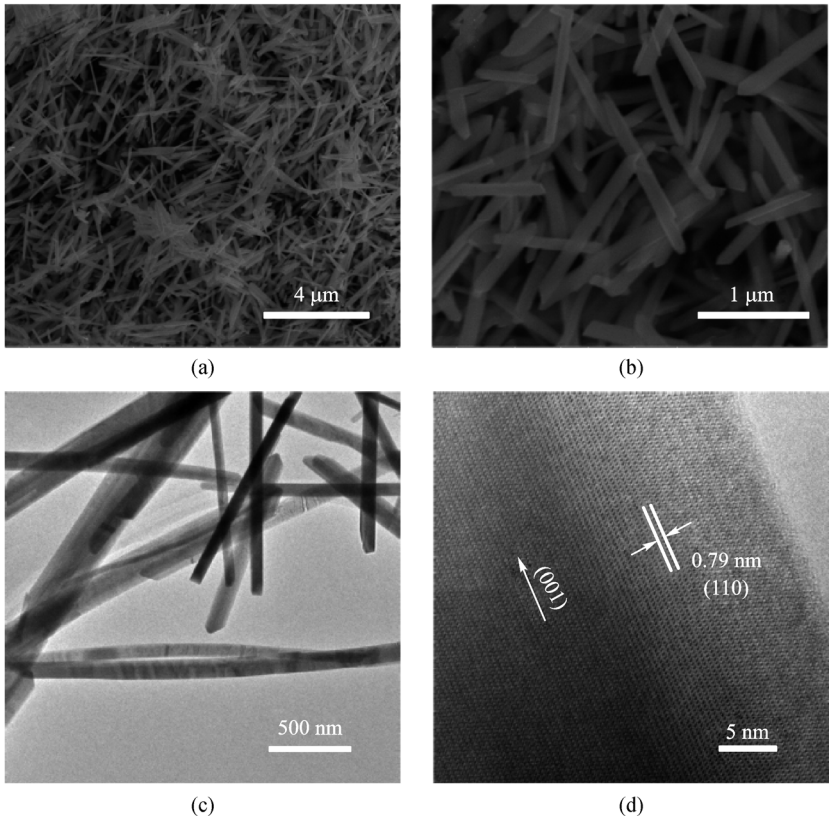

Fig. 2 (a) and (b) typical SEM images of Bi_2S_3 nanorods; (c) and (d) TEM image and HRTEM image of Bi_2S_3 nanorods, respectively

3.3 Photoresponse properties of Bi_2S_3 nanorods

As we all know, photoelectrical switches and photodetectors are widely used in imaging techniques, optical communications [34]. Generally, conventional photodetectors are usually in film or bulk configurations, which mean higher power consumption compared with the photodetectors constructed by micro- or nano-scale materials. Therefore, Bi_2S_3 nanorods were chosen as a representative micro- and nano- materials to evaluate the potential application in photodetectors. The photodetectors constructed with Au interdigital electrode and Bi_2S_3 nanorods were shown in the inset of Fig. 3(a). Evidently, the *I-V* curves were presented as linear whether the photoconductors were exposed to light or in dark, as shown in Fig. 3(a). Therefore, we can conclude that the contact between Bi_2S_3 and Au were ohmic-type. A distinct light current was observed when the photodetectors were exposed in light, demonstrating these Bi_2S_3 nanorods have an excellent photovoltaic response upon light illumination. It is evidently shown that the photocurrent is increased with the increase of bias voltage. According to the formula of photocurrent,

$$I_{\mathrm{ph}} = \frac{U\Delta\sigma A}{L},$$

where U is the bias voltage, L is the length of photodetector, A is the sectional area, $\Delta\sigma$ is the photoconductivity. As can be seen from the formula, I_{ph} is proportional to the bias voltage. And our results also proved this point, as shown in Fig. 3(b). Based on the formula of the transit time of electrons,

$$t_{\mathrm{m}} = \frac{L}{\mu_{\mathrm{n}} U},$$

where L is the length of photoconductor, μ_{n} is the mobility of electrons and U is the bias voltage. We can conclude that electrons have a higher mobility, their transit time is short than τ (carrier lifetime) from the formula above. So the separation of photo-generated electrons and holes is more efficient in a high bias. In addition, the light current significantly increases approximately 2 orders of magnitude compared with the dark state as shown in Figs. 3(a) and 3(b), indicating excellent optical sensitivity. Good photoresponse property should result from the increased charge carrier concentration via direct electron-hole pair

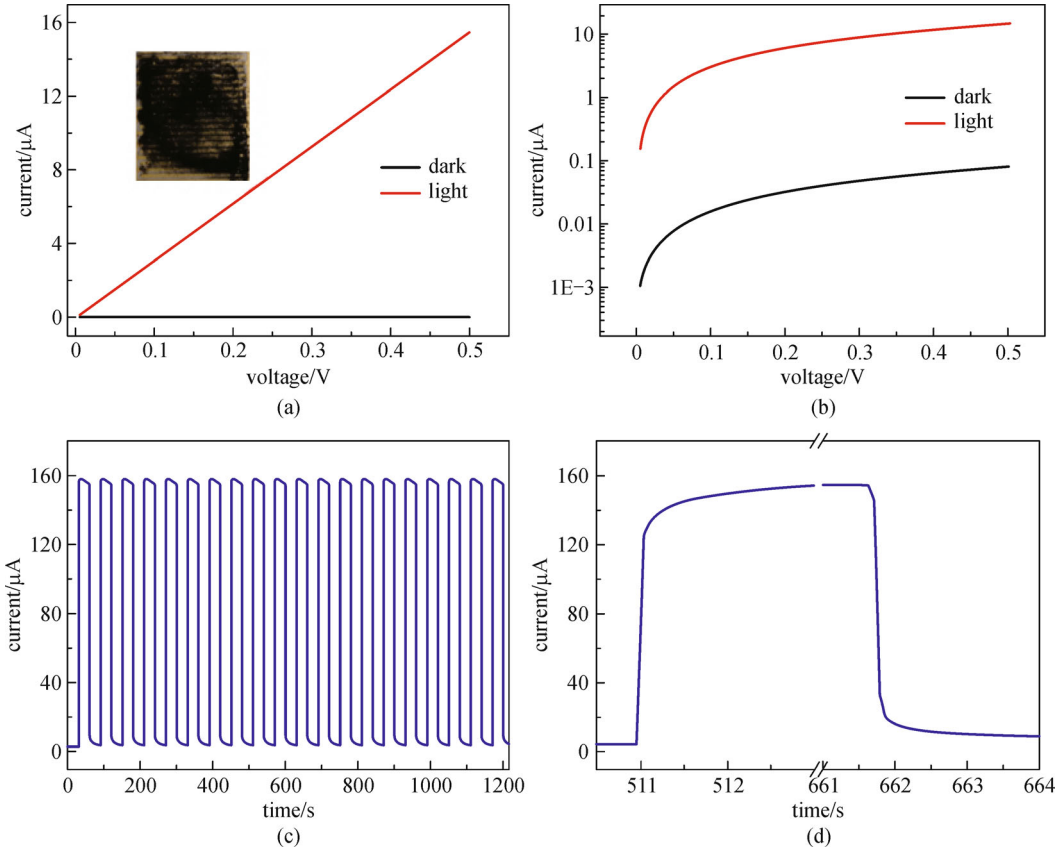

Fig. 3 Photoresponsive sensitivity of the Bi_2S_3 nanorods as a representative system was studied. (a) *I-V* characteristic of device in the dark and under simulated A M 1.5 illumination; (b) logarithmic plot of (a); (c) time dependence of current of Bi_2S_3 micro-flower at a bias of 5 V in the dark and under simulated A M 1 illumination; (d) enlarged portion of the 510–513 s and 661–664 s

generation under light illumination and the enhanced conductivity of Bi_2S_3. Figure 3(c) depicts the photoresponse as a function of time with the light regularly chopped at a bias of 5 V to reveal the stability and response capability. The photocurrent quickly reaches to a maximum value (the steady-state), and then rapidly returned to its initial ones (the normal state) once the light was turned off, revealing the Bi_2S_3 nanorods respond quickly to the light. Such on-off cycles were repeated several times without any distinguishable degradation, showing its excellent stability and reproducible behavior. The response time is generally defined as the time required to recover from 10% to 90% of the maximum photocurrent. The recovery time has similar definition. The response and recovery time at a bias of 5 V for our photodetector are calculated to be 371.66 and 386 ms, respectively. The above results indicate that the photodetectors based on Bi_2S_3 nanorods have a good stability and responds quickly to light, suggesting promising applications of Bi_2S_3 microflower in photoelectrical switches and photodetectors. More importantly, the Bi_2S_3 nanorods as well as the relevant photosensitive devices presented in this paper were very easy to fabricate and no complex equipment and procedures are needed. Thus, this method offers probability for low-cost and large-scale applications in the integration circuits.

4 Conclusions

In summary, we have successfully synthesized Bi_2S_3 nanorodsvia a facile, low-cost, and low power consumption while effective one-pot solution-based method. And we also investigated the photosensitivity properties based on Bi_2S_3 nanorods in an ambient environment. It is worth noting that the light current significantly increases by 2 times compared with the dark state. The devices based on Bi_2S_3 nanorods show an excellent stability and fast response to the light as well. These findings indicate these nanorods may have great potential applications in high speed and high-sensitivity photoelectrical switches and light sensitive devices.

Acknowledgements This work was supported by the National Basic Research Program of China (Nos. 2012CB619302 and 2010CB923204), the Science and Technology Bureau of Wuhan City (No. 2014010101010006), Natural Science Foundation of Hubei Province (No. 2011CDA81), Science Foundation from Hubei Provincial Department of Education (No. D20131001), the National Natural Science Foundation of China (Grant Nos. 10990103, 51002058, 61274010 and 61405076) and the Science and Technology Project of Zhejiang Province (No. 2012C33057).

References

1. Chen Y C, Cao T, Chen C, Pedramrazi Z, Haberer D, de Oteyza D G, Fischer F R, Louie S G, Crommie M F. Molecular bandgap engineering of bottom-up synthesized graphene nanoribbon heterojunctions. Nature Nanotechnology, 2015, 10(2): 156–160
2. Rao P M, Cai L, Liu C, Cho I S, Lee C H, Weisse J M, Yang P, Zheng X. Simultaneously efficient light absorption and charge separation in $WO_3/BiVO_4$ core/shell nanowire photoanode for photoelectrochemical water oxidation. Nano Letters, 2014, 14(2): 1099–1105
3. Peng S, Li L, Wu H B, Madhavi S, Lou X W. Controlled growth of NiMoO4 nanosheet and nanorod arrays on various conductive substrates as advanced electrodes for asymmetric supercapacitors. Advanced Energy Materials, 2015, 5(2): 1401172
4. Tan C, Qi X, Huang X, Yang J, Zheng B, An Z, Chen R, Wei J, Tang B Z, Huang W, Zhang H. Single-layer transition metal dichalcogenide nanosheet-assisted assembly of aggregation-induced emission molecules to form organic nanosheets with enhanced fluorescence. Advanced Materials, 2014, 26(11): 1735–1739
5. Huang X, Yu H, Chen J, Lu Z, Yazami R, Hng H H. Ultrahigh rate capabilities of lithium-ion batteries from 3D ordered hierarchically porous electrodes with entrapped active nanoparticles configuration. Advanced Materials, 2014, 26(8): 1296–1303
6. Giri A K, Pal P, Ananthakumar R, Jayachandran M, Mahanty S, Panda A B. 3D hierarchically assembled porous wrinkled-paper-like structure of $ZnCo_2O_4$ and Co-ZnO@C as anode materials for lithium-ion batteries. Crystal Growth & Design, 2014, 14(7): 3352–3359
7. Cheng C, Ren W, Zhang H. 3D TiO_2/SnO_2 hierarchically branched nanowires on transparent FTO substrate as photoanode for efficient water splitting. Nano Energy, 2014, 5: 132–138
8. Choy J H, Jang E S, Won J H, Chung J H, Jang D J, Kim Y W. Soft solution route to directionally grown ZnOnanorodarrays on Si wafer; room-temperature ultraviolet laser. Advanced Materials, 2003, 15(22): 1911–1914
9. Huang H, Pan L, Lim C K, Gong H, Guo J, Tse M S, Tan O K. Hydrothermal growth of TiO_2 nanorod arrays and in situ conversion to nanotube arrays for highly efficient quantum dot-sensitized solar cells. Small, 2013, 9(18): 3153–3160
10. Liao J Y, Lei B X, Chen H Y, Kuang D B, Su C Y. Oriented hierarchical single crystalline anatase TiO_2 nanowire arrays on Ti-foil substrate for efficient flexible dye-sensitized solar cells. Energy & Environmental Science, 2012, 5(2): 5750–5757
11. Guo W, Xu C, Wang X, Wang S H, Pan C, Lin C, Wang Z L. Rectangular bunched rutile TiO_2 nanorodarrays grown on carbon fiber for dye-sensitized solar cells. Journal of the American Chemical Society, 2012, 134(9): 4437–4441
12. Tang Z R, Li F, Zhang Y, Fu X, Xu Y J. Composites of titanatenanotube and carbon nanotube as photocatalyst with high mineralization ratio for gas-phase degradation of volatile aromatic pollutant. Journal of Physical Chemistry C, 2011, 115(16): 7880–7886
13. Jiang J, Li Y, Liu J, Huang X. Building one-dimensional oxide nanostructure arrays on conductive metal substrates for lithium-ion battery anodes. Nanoscale, 2011, 3(1): 45–58
14. Wang Z L, Song J. Piezoelectric nanogenerators based on zinc oxide nanowire arrays. Science, 2006, 312(5771): 242–246

15. Martinez L, Bernechea M, de Arquer F P G, Konstantatos G. Near IR-sensitive, non-toxic, polymer/nanocrystalsolar cells employing Bi_2S_3 as the electron acceptor. Advanced Energy Materials, 2011, 1 (6): 1029–1035
16. Xiao G, Dong Q, Wang Y, Sui Y, Ning J, Liu Z, Tian W, Liu B, Zou G, Zou B. One-step solution synthesis of bismuth sulfide (Bi_2S_3) with various hierarchical architectures and their photoresponse properties. RSC Advances, 2012, 2(1): 234–240
17. Li Y, Wei F, Ma Y, Zhang H, Gao Z, Dai L, Qin G. Selected-control hydrothermal synthesis and photoresponse properties of Bi_2S_3micro/nanocrystals. CryEngComm, 2013, 15(33): 6611–6616
18. Konstantatos G, Levina L, Tang J, Sargent E H. Sensitive solution-processed Bi_2S_3 nanocrystalline photodetectors. Nano Letters, 2008, 8(11): 4002–4006
19. Yao K, Gong W W, Hu Y F, Liang X L, Chen Q, Peng L M. Individual Bi_2S_3 nanowire-based room-temperature H_2 sensor. Journal of Physical Chemistry C, 2008, 112(23): 8721–8724
20. Bao H, Li C M, Cui X, Gan Y, Song Q, Guo J. Synthesis of a highly ordered single-crystalline Bi_2S_3 nanowire array and its metal/semiconductor/metal back-to-back Schottky diode. Small, 2008, 4 (8): 1125–1129
21. Ma J, Liu Z, Lian J, Duan X, Kim T, Peng P, Liu X, Chen Q, Yao G, Zheng W. Ionic liquids-assisted synthesis and electrochemical properties of Bi_2S_3 nanostructures. CrystEngComm, 2011, 13(8): 3072–3079
22. Rabin O, Manuel Perez J, Grimm J, Wojtkiewicz G, Weissleder R. An X-ray computed tomography imaging agent based on long-circulating bismuth sulphide nanoparticles. Nature Materials, 2006, 5(2): 118–122
23. Schricker A D, Sigman M B Jr, Korgel B A. Electrical transport, Meyer–Neldel rule and oxygen sensitivity of Bi_2S_3 nanowires. Nanotechnology, 2005, 16(7): S508–S513
24. Liao X H, Wang H, Zhu J J, Chen H Y. Preparation of Bi_2S_3 nanorods by microwave irradiation. Materials Research Bulletin, 2001, 36(13–14): 2339–2346
25. Tang C J, Wang G Z, Wang H Q, Zhang Y X, Li G H. Facile synthesis of Bi_2S_3 nanowire arrays. Materials Letters, 2008, 62(21–22): 3663–3665
26. Tang C, Wang C, Su F, Zang C, Yang Y, Zong Z, Zhang Y. Controlled synthesis of urchin-like Bi_2S_3 via hydrothermal method. Solid State Sciences, 2010, 12(8): 1352–1356
27. Lu F, Li R, Li Y, Huo N, Yang J, Li Y, Li B, Yang S, Wei Z, Li J . Improving the field-effect performance of Bi_2S_3 single nanowires by an asymmetric device fabrication. A European Journal of Chemical Physics and Physical Chemistry, 2015, 16(1): 99–103
28. Andzane J, Kunakova G, Varghese J, Holmes J D, Erts D. Photoconductive properties of Bi_2S_3 nanowires. Journal of Applied Physics, 2015, 117(6): 064305
29. Wang H, Zhu J J, Zhu J M, Chen H Y. Sonochemical method for the preparation of bismuth sulfide nanorods. Journal of Physical Chemistry B, 2002, 106(15): 3848–3854
30. Wei F, Zhang J, Wang L, Zhang Z K. Solvothermal growth of single-crystal bismuth sulfide nanorods using bismuth particles as source material. Crystal Growth & Design, 2006, 6(8): 1942–1944
31. Peng X S, Meng G W, Zhang J, Zhao L X, Wang X F, Wang Y W, Zhang L D. Electrochemical fabrication of ordered Bi_2S_3 nanowire arrays. Journal of Physics D, Applied Physics, 2001, 34(22): 3224–3228
32. Zhang B, Ye X, Hou W, Zhao Y, Xie Y. Biomolecule-assisted synthesis and electrochemical hydrogen storage of Bi_2S_3 flowerlike patterns with well-aligned nanorods. Journal of Physical Chemistry B, 2006, 110(18): 8978–8985
33. Wang Y, Chen J, Wang P, Chen L, Chen Y B, Wu L M. Syntheses, growth mechanism, and optical properties of [001] growing Bi_2S_3 nanorods. Journal of Physical Chemistry C, 2009, 113(36): 16009–16014
34. Kind H, Yan H, Messer B, Law M, Yang P. Nanowire ultraviolet photodetectors and optical switches. Advanced Materials, 2002, 14 (2): 158–160

Taotao Ding received the B.S. degree from School of Environmental and Chemical Engineering, Nanchang Hangkong University, China, in 2011. Now, he is working toward his Ph.D. degree in Wuhan National Laboratory for Optoelectronics, Huazhong University of Science and Technology, China. His research interests include synthesis of nano-materials and their application in sensors and energy storage.

Yu Tian is a lecturer in School of Physics and Information Engineering, Jianghan University, China. She received the B.S. degree from Physics and Electronic Science Department, Luoyang Normal University, China, in 2004; and received the M.S.-Ph.D. degrees from Materials Physics and Chemistry, Wuhan University, China, in 2010. From 2010 − 2012, she was a postdoctor in Wuhan National Laboratory for Optoelectronics, Huazhong University of Science and Technology, China. Her research interests include synthesis of ZnO nanowire and investigation of the defect in ZnO nanowire.

Jiangnan Dai is an associate professor in Wuhan National Laboratory for Optoelectronics, Huazhong University of Science and Technology, China. He received the B. S. degree from Hunan University of Science and Technology, China, in 2002; received the M.S. and Ph.D. degrees from School of Materials Science and Engineering, Nanchang University, China, in 2004 and 2007 respectively. From 2008 − 2010, he was a postdoctor in Wuhan National Laboratory for Optoelectronics, Huazhong University of Science and Technology, China. His research focuses on material growth and device fabrication of wide bandgap semiconductor (AlGaN, GaN, ZnO).

Changqing Chen is a proferssor in Wuhan National Laboratory for Optoelectronics, Huazhong University of Science and Technology, China. He received the B.S. and M. S. degrees from Wuhan University, China, in 1992 and 1994 respectively; received the Ph.D. degrees from Shanghai Institute of Metallurgy, Academy of Sciences of China, China (in 1997) and University of Erlangen-Nürnberg, German (in 2000). From 2001 − 2004, he was a research scientist in Virginia Commonwealth University and University of South Carolina. His research focuses on semiconductors materials and devices including light-emitting diodes and photodetectors.